AIAA 90-2594
Hall Current Ion Thruster Performance

K. Komurasaki and Y. Arakawa
University of Tokyo
Tokyo, Japan

AIAA/DGLR/JSASS
21st International Electric Propulsion Conference
July 18-20, 1990 / Orlando, FL

Hall Current Ion Thruster Performance

Kimiya Komurasaki[*] and Yoshihiro Arakawa[†]
Department of Aeronautics, University of Tokyo
7-3-1 Hongo, Bunkyo-ku, Tokyo 113, Japan

Abstract

A Hall current ion thruster has been developed to investigate its thruster performance and acceleration process. Thrust was measured by mounting the thruster on a pendulum type thrust stand and internal efficiencies such as propellant utilization, acceleration and beam energy efficiencies were measured with an ion beam collector and an ion energy analyzer to examine their relations with the thruster performance. As the result, it was found that the product of such internal efficiencies gave a good approximation to the thrust efficiency directly obtained from thrust measurement and that the acceleration efficiency was the most important factor to be increased for the improvement of thruster performance. Until now maximum thrust efficiency of 32 % was obtained at a specific impulse of 1300 sec when xenon was used as the propellant.

Nomenclature

e : electronic charge
f : energy distribution function
g : gravitational acceleration
I_a : acceleration current
I_b : ion beam current
I_e : backstreaming electron current
I_p : ion production current
I_{sp} : specific impulse
$\dot{m}$: propellant flow rate
M : ion mass
T : thrust
V : ion beam energy
V_a : acceleration voltage
V_m : average ion beam energy
α : ion loss fraction
β : coefficient of ion production
η_a : acceleration efficiency
η_E : ion beam energy efficiency
η_T : thrust efficiency
η_u : propellant utilization

Introduction

A Hall current ion thruster has a coaxial channel in which radial magnetic fields are applied to maintain a high voltage between anode and cathode neutralizer, and ions generated there are accelerated downstream to produce thrust. As the channel is filled with quasi-neutral plasma, there is no space charge limited current and hence this type of thruster has a capability of producing much higher thrust density than conventional ion thrusters. Besides, it enables one to choose various propellant gases and acceleration voltage appropriate for a given specific impulse.

Although MPD and conventional ion thrusters are excellent propulsion functions for space mission, both have difficult problems to overcome, particularly in their life times. On MPD thrusters, electrodes may be eroded due to their extremely high discharge current. In case of conventional ion thrusters, acceleration grids are easily spattered by ions that are produced with charge-exchanged collisions. In contrast, Hall current ion thrusters are generally operated with a moderate current and with a moderate voltage so that no such erosion problems may be induced.

Hall current ion thrusters have been studied and developed in several countries,[1-4] but most of them have been made to understand physical phenomena in plasma acceleration processes and few have produced high thruster performance comparable to the other types of thrusters. The object of this study is to improve Hall current ion thruster performance and acceleration processes through the experimental investigation of its performance characteristics and acceleration process.

Experimental apparatus and procedures

Hall current ion thrusters used in this work are illustrated in Fig. 1. Each thruster consists of anode, cathode neutralizer and acceleration channel in which a radial magnetic field is applied. Two thin ceramic cylinders are inserted in the acceleration channel to prevent inner and outer metal walls from short-circuiting plasmas. The cathode neutralizer located downstream of the channel supplies electrons not only to ionize propellant gases in the channel but also to neutralize ion beam extracted out downstream. In Thruster I, a plasma source called periplasmatron is employed to produce ions particularly in the upstream part of the channel for efficient ion acceleration. Using the magnetic circuit formed by solenoidal coils and magnetic pole pieces, the magnetic field can be applied in the radial direction up to 200 gauss on the acceleration channel while it is maintained under 50 gauss in the ion production zone. On the other hand, Thruster II has a shorter acceleration channel with stronger magnetic fields of up to 1000 gauss. Propellant is fed to the channel through 12 holes in the anode. The cross section area of the acceleration channel is almost the same as that of Thruster I.

---

*) Graduate Student.
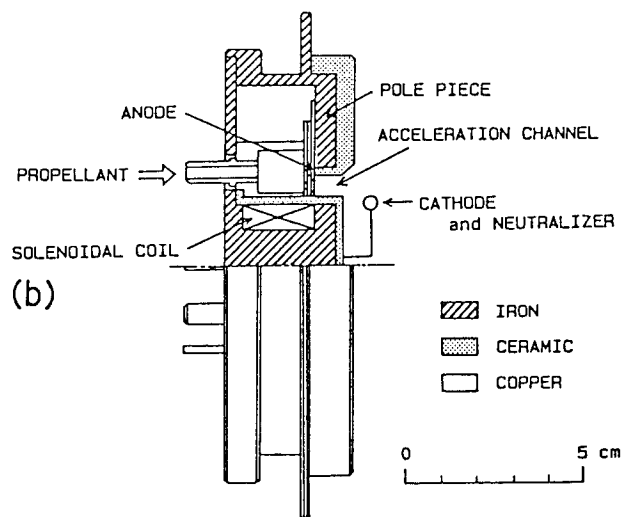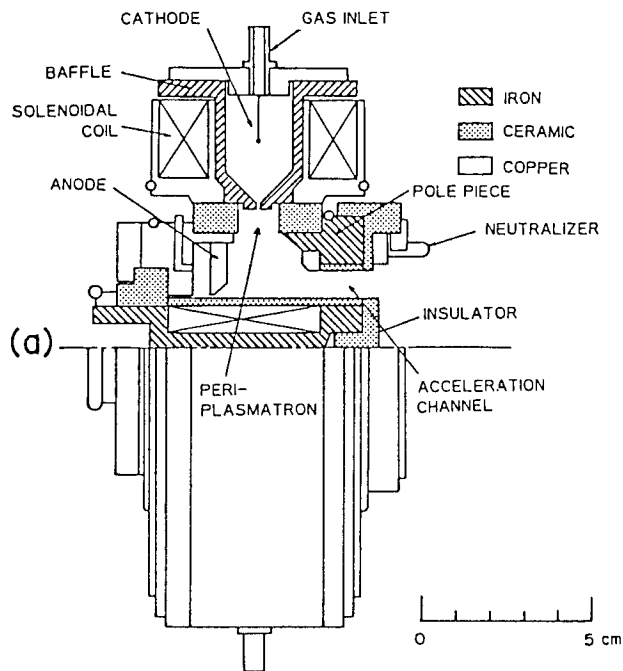†) Associate Professor, Member AIAA.

Fig. 1 Hall current ion thrusters:
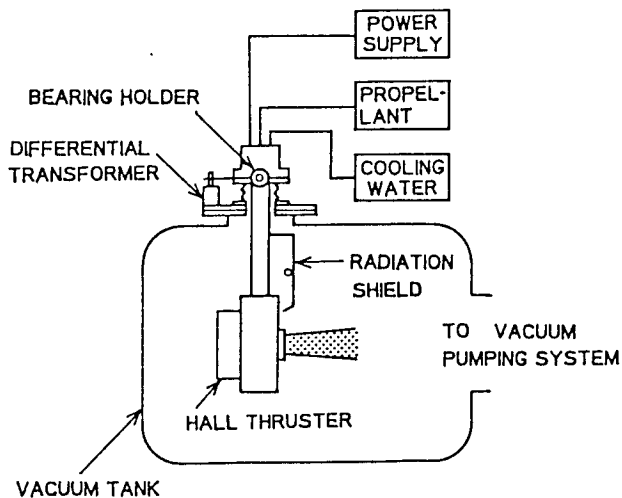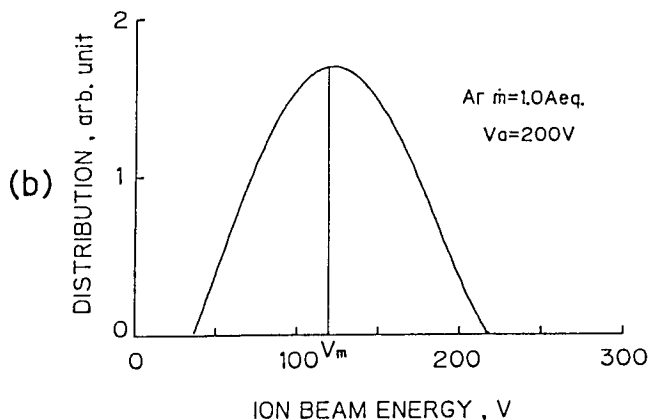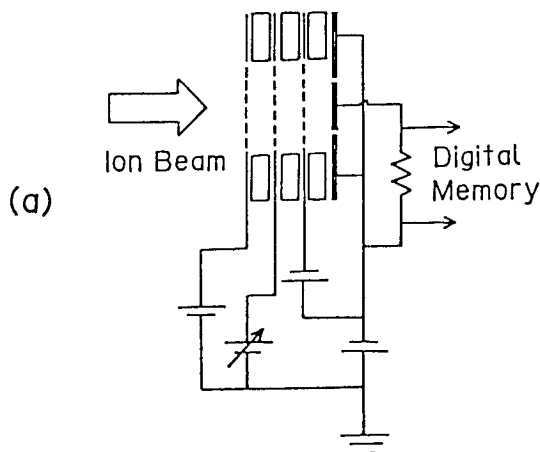(a) Thruster I and (b) Thruster II

Fig. 2 Pendulum-type thrust stand

Fig. 3 (a) Multi-grid ion energy analyzer
and (b) example of energy distribution

To measure thrust, the thruster is mounted on a pendulum type thrust stand, as shown in Fig. 2. It utilizes vacuum bellows and radial bearings. The vertical position of the fulcrum is adjustable, allowing the atmospheric pressure and the weight of the stand to be supported by bellows. Hence, no radial load is exerted on the bearings, eliminating the effect of the friction force at the bearings on thrust measurement. Deflection of the thrust stand was sensed by a linear differential transformer. One of the most difficult problems on thrust measurement is the appearance of drift in signals during the thruster operation. In order to eliminate such a drift, the thrust stand was shielded from the exhaust plume with a water-cooled copper plate not

to be distorted by heat radiation of the exhaust plume. The accuracy of thrust was kept less than 1 mN.

Extracted ion beam current was measured with an ion beam collector which was located 10 cm downstream of the thruster exit. A multi-grid energy analyzer, composed of three fine mesh grids and a negatively-biased collector, was fabricated to measure energy distributions of the extracted ion beam (see Fig. 3(a)). The energy distribution can be obtained to observe ion current to the collector as a function of retarding bias voltage imposed on the second grid. A typical example of energy distribution is illustrated in Fig. 3(b). Average ion beam energy can be calculated from this energy distribution.

To investigate the ion production and acceleration processes in the acceleration channel, plasma properties such as electron temperature, plasma density and plasma potential were measured using cylindrical Langmuir probes inserted into the channel and scanned in both radial and axial directions.

Experiments were conducted in a 0.8 m-diameter and 2.5 m-long vacuum chamber which was evacuated by a 22 inch diffusion pump backed by a root blower and rotary pumps. The chamber pressure was maintained under 2×10^{-4} Torr for most of the operating conditions.

Results and Discussion

From the thrust measurement, one can calculate specific impulse, I_{sp}, and thrust efficiency, η_T, using the well-known relations as given by

$$I_{sp} = \frac{T}{\dot{m}g} \tag{1}$$

and

$$\eta_T = \frac{T^2}{2\dot{m}I_aV_a} \tag{2}$$

Here, T is thrust, $\dot{m}$ is the propellant mass flow rate, g is the gravitational acceleration, I_a and V_a are the acceleration current and voltage, respectively. Neither excitation power for solenoidal coils nor heating power of cathode filaments is taken into account on the calculation of thrust efficiency, since, for practical case, solenoidal coils may be replaced by permanent

magnets and cathode filaments by hollow cathode. In the experiment using Thruster I, the periplasmatron worked as not a plasma source but as an igniter, since no improvement in thrust efficiency has been observed. This is considered that the curved magnetic field lines formed in the upstream region of the acceleration channel prevent ions produced in the periplasmatron being extracted as ion beams.

To investigate thruster performance characteristics, the following internal efficiencies are introduced and defined by the equations

$$\eta_u = \frac{MI_b}{e\dot{m}} \tag{3}$$

$$\eta_a = \frac{I_b}{I_a} \tag{4}$$

$$\eta_E = \frac{V_m}{V_a} \tag{5}$$

where η_u is propellant utilization, η_a acceleration efficiency, η_E beam energy efficiency, M ion mass, e electronic charge, I_b the ion beam current and V_m average ion beam energy calculated from the ion energy distribution, and is given by

$$V_m = \left(\int f(V)\sqrt{V}dV \right)^2 \tag{6}$$

Here, f(V) is the energy distribution function and V is ion beam energy. Assuming that all ions produced are singly-charged, thrust can be written by

$$T = I_b\sqrt{2MV_m/e} \tag{7}$$

Substituting Eqs. (3)-(7) into Eq. (2), the thrust efficiency yields

$$\eta_T = \eta_u\eta_a\eta_E \tag{8}$$

Typical examples of such internal efficiencies and thrust efficiencies for several operating conditions are listed in Table 1. When argon is used as the propellant, the propellant utilization increases as either acceleration voltage or propellant flow rate increases. However, the maximum utilization is about 50 %, which is about a half of that with xenon propellant. This seems reasonable since xenon gases are more easily ionized than argon gases.

Table 1 Operating parameters and efficiencies obtained by Thruster I

$\dot{m}$ (Aeq.)		V_a (V)	I_a (A)	I_b (A)	η_a (%)	η_u (%)	η_E (%)	η_T^* (%)	η_T (%)
Ar	0.75	200	0.45	0.10	22	13	63	1.8	1.0
	1.00	175	0.97	0.22	23	22	60	3.0	3.3
	1.00	200	1.24	0.29	23	29	60	4.0	4.9
	1.00	225	1.49	0.36	24	36	63	5.4	6.9
	1.00	250	1.70	0.42	25	42	63	6.6	7.0
	1.25	200	1.85	0.50	27	40	60	6.5	7.0
	1.75	200	3.08	0.92	30	52	63	9.8	11.2
Xe	0.30	150	0.82	0.23	28	77	66	14	12
	0.50	100	1.49	0.37	25	74	65	12	13
	0.50	130	1.40	0.38	27	76	65	13	16
	0.50	150	1.45	0.40	28	80	62	14	15
	0.70	150	2.21	0.65	29	97	62	17	15

*) Thrust efficiency calculated by Eq. (8)

The beam energy efficiencies ranged from 60 % to 66 % for most of the operating conditions and were unchanged even when either acceleration voltage or propellant flow rate was changed. The acceleration efficiency was low and ranged from 22 % to 30 %. This value is much lower than the other efficiencies, which eventually leads to a low thrust efficiency.

Comparisons of the thrust efficiency obtained from thrust measurement with that derived from the product of internal efficiencies are also shown in Table 1. The result shows a fair agreement between in their values.

From the measurement of the internal efficiencies, it was found that the acceleration efficiency is the most predominant factor for determining thrust efficiency. To evaluate the acceleration efficiency in detail, a simple model is presented as follows.

In the acceleration channel, ions are produced by ionization collisions of electrons with neutral atoms. Ion production current in the channel, I_p, is given by

$$I_p = \beta I_e \qquad (9)$$

where I_e is electron current backstreaming from the cathode neutralizer to the anode and a coefficient β is a quantity that expresses how efficiently ions are produced. As volume recombination can be neglected as small, the ions produced in the channel are either lost to the inner and outer walls or exhausted downstream of the channel. Hence, ion beam current, I_b, is given by

$$I_b = (1-\alpha)I_p \qquad (10)$$

where, α denotes a fraction of ions produced that are lost to the wall.

The sum of the ion beam current and the backstreaming electron current is equal to the acceleration current as

$$I_a = I_b + I_e \qquad (11)$$

Substituting Eqs. (9)-(11) into Eq. (4), the acceleration efficiency can be expressed as functions of both α and β.

$$\eta_a = \frac{\beta(1-\alpha)}{\beta(1-\alpha)+1} \qquad (12)$$

From this equation, it is found that, to obtain a high acceleration efficiency, ion loss fraction should be as low as possible, together with an effort of efficient ion production. Among these parameters, β is considered to be influenced by operating parameters as propellant flow rate and acceleration voltage, while α will be determined from geometric design parameters as acceleration channel length, cross-sectional area, and magnetic field configuration. Actually, the improvement of acceleration efficiency could be achieved with a choice of operating condition change to a higher propellant flow rate and to a higher acceleration voltage, as seen in Table 1, and of a shorter acceleration channel with a higher magnetic field strength, as described later.

The plasma diagnostics in the acceleration channel were performed using the Langmuir probes. In the upstream region as shown in Fig. 4, which extends from the anode to the middle of channel, the magnetic field has a relatively low strength (below 50 gauss) and curved lines of force, while in the downstream region, which extends from the

middle of channel to the exit, the field lines are closely arranged (that is, a high field strength) and are almost perpendicular to the axis.

Figure 5 shows distributions of the plasma potential, electron temperature and electron density on the condition where the acceleration voltage is 200 V, the acceleration current 1.3 A and the argon flow rate 1.0 Aeq. As seen in Fig. 5(a), the shape of equipotential lines is similar to that of the magnetic field lines. This result is due to that equipotential lines are formed along the magnetic field lines as electrons move much more easily along the field lines than across them. The electron temperature has a peak of around 10 eV at the position where the magnetic field strength is maximum, as seen in Fig. 5(b). This trend is also seen in the experiment conducted by Bishaev et al.[6]
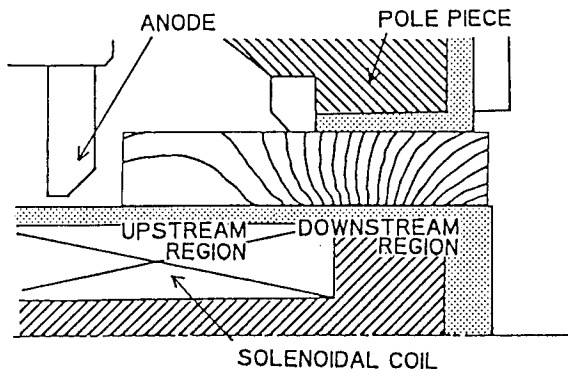

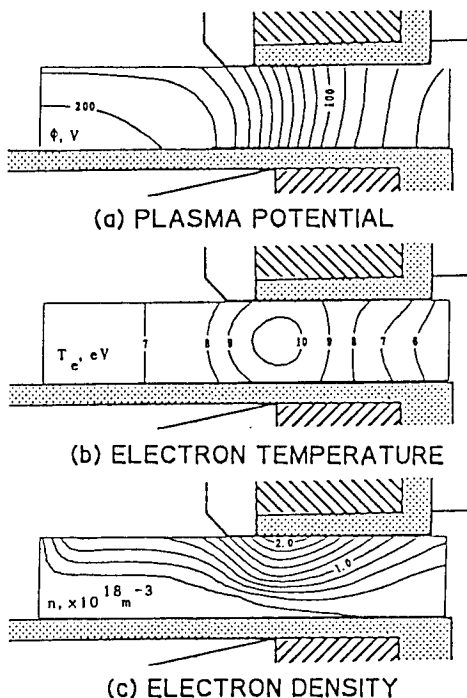Fig. 4 Magnetic field configuration in the acceleration channel

Fig. 5 Distributions of (a) plasma potential, (b) electron temperature, and (c) electron density

4

To examine the ion production and the acceleration process in more detail, the ion production rate and the beam trajectory were calculated from the measured profiles of electron temperature, electron density and plasma potential, assuming that ions are produced by ionization collisions of the Maxwellian electrons with neutral atoms and then are electrostatically accelerated by electric fields without any collision. As shown in Fig. 6(a), the highest ion production rate was obtained near the outer wall in the middle of channel. Using this result, the total ion production current in the channel was estimated 1.3 A. Figure 6(b) illustrates the domains related to ion beam extraction; ions produced in the dotted region, are exhausted as ion beams and ions produced in the other region are lost to the walls. As seen in this figure, most of the ions produced in upstream region are lost to the wall by the electric field distortion caused by the curve magnetic field lines while the ions produced in downstream region are accelerated to produce ion beams by the axial electric fields. From the result, about two thirds of ions produced in the acceleration channel were estimated to be lost to the wall. This fraction corresponds to the ion loss fraction $\alpha = 0.67$, which results in a relatively low acceleration efficiency. Actually, the acceleration efficiency obtained from the ion beam current measurement was 0.32 which is a fair agreement with that calculated by Eq. (12), provided that $\beta = 1$. When the ion loss fraction were reduced to 0.2, 44 % acceleration efficiency would be obtained.

(a) ION PRODUCTION

$q, \times 10^{24} \, m^{-3} \, s^{-1}$
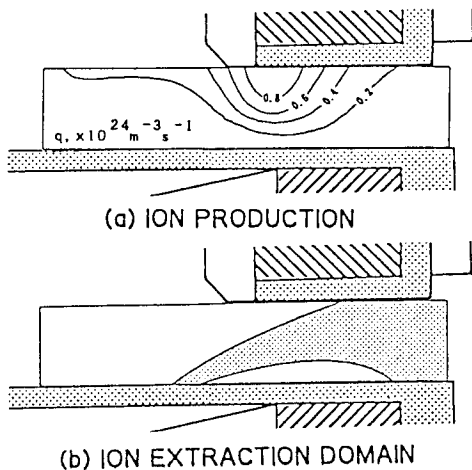
(b) ION EXTRACTION DOMAIN

Fig. 6 (a) Ion production distribution and (b) ion extraction domain

As described in the previous section, the acceleration efficiency was found to be the most predominant factor for the improvement of thruster performance and is required to increase through the reduction of ion loss fraction to the wall surfaces. In order to reduce ion loss fraction, the acceleration channel should be shortened together with the arrangement of magnetic field lines to be perpendicular to the axis. However, shortening the acceleration channel brings an increase in backstreaming electron current and hence a decrease in acceleration efficiency.

Therefore, stronger magnetic field is required to preserve the integral of magnetic field strength along the acceleration channel.[7] From this point of view, Thruster II was designed and tested to examine its performance.

Figure 7 shows the thruster performance obtained by Thruster II. The thrust efficiencies increase with specific impulse, attain their peaks around $I_{sp} = 1300$ sec and then decrease with a further increase of I_{sp}. As the specific impulse increases with acceleration current, the increase in thrust efficiency with I_{sp} can be explained as the result of the increase of propellant utilization, regarding that both the acceleration efficiency and the beam energy efficiency are relatively insensitive to acceleration current. As seen in this figure, the thrust efficiencies have their peaks on the propellant utilization of around 90 %. As the specific impulse increases furthermore, the propellant utilization defined by Eq. (3) exceeds 100 %, indicating to the presence of doubly-charged ions. If doubly-charged ions were produced at the same position as singly-charged ones, they would be accelerated to have 1.4 times the velocity of singly-charged ions. Such a velocity difference between singly-charged and doubly-charged ions results in the decrease of thrust efficiency, since the beam kinetic energy appeared on Eq. (2) is not equal to the sum of kinetic energy of each particle but is the kinetic energy derived from the average ion velocity. Moreover, it was observed that the thrust efficiency increases with propellant flow rate. This is because the acceleration efficiency increases with propellant flow rate. As ions are usually more effectively produced with the increase of neutral density, β increases with propellant flow rate for a given propellant utilization. From Eq. (12) this leads to the improvement of acceleration efficiency. As the result, the maximum thrust efficiency of 32 % could be obtained at the highest propellant flow rate of the present experiment.

Similar trends were obtained with argon propellant as shown in Fig. 8. The thrust efficiency increases both with specific impulse and propellant flow rate. However, the maximum thrust efficiency was only 15 %, which is about a half of that with xenon propellant. Such a low thrust efficiency with argon is largely caused by the low propellant utilization. Therefore, it will be necessary for the improvement of thruster performance to produce ions in the upstream region of the acceleration channel by means of such a plasma source as periplasmatron and then to introduce them efficiently into the acceleration channel.

Aside from this point, the thrust efficiencies obtained by Thruster II could be raised about twice those of Thruster I. The maximum thrust was up to 22 mN, which corresponds to a thrust density of 2.5 mN/cm² in the acceleration channel, being two orders higher than that of conventional ion thrusters.

Conclusion

Thruster performance in Hall current ion thrusters was investigated by measuring thrust, ion beam current and ion beam energy. From these measurements, it was found that the product of propellant utilization, acceleration and beam energy efficiencies gives a good approximation to

the thrust efficiency directly obtained from the thrust measurement, and that the acceleration efficiency is the most important factor to increase for the improvement of thruster performance.

Plasma diagnostics was performed to investigate the ion production and loss processes inside the acceleration channel. The results have shown that the ion loss to the walls was caused by distorted electric fields that originate from the curved magnetic field lines, and that the high ion loss fraction leads to poor acceleration efficiencies.

To improve thruster performance by reducing the ion loss fraction to the wall, Thruster II which has a short acceleration channel applied with strong magnetic fields was designed. As the result, the acceleration efficiency could be improved up to 40 % and the maximum thrust efficiency of 32 % was obtained at a specific impulse of 1300 sec when xenon was used as the propellant.

References

1. Koehne, R., Lindner, F., Schreitmueller, K. R., Wichmann, H. G. and Zeyfang E., "Further Investigation on Low-Density Hall Accelerators," AIAA Journal, Vol. 8, No. 5, 1970, pp. 873-879.
2. Morozov, A. I., Esipchuk, Yu. V.,Ticinin, G. N.,Trofinov, A. V., Sharov, Yu. A. and Shahepkin, G. Ya., "Plasma Acceleration with Closed Electron Drift and Extended Acceleration Zone," Soviet Physics-Technical Physics, Vol. 17, 1972, pp. 38-45.
3. Patterson, M. J., Robinson, R. S., Schemmel, T. D. and Burgess, D. R., "Experimental Investigation of a Closed-Drift Thruster," AIAA Paper 85-2060, 1985.
4. Yamagiwa, Y. and Kuriki, K., "Experimental Study of Double Stage Discharge Hall Ion Thruster," Proceedings of 20th International Electric Propulsion Conference, 1988, pp. 530-534.
5. Sasoh, A., Solem, A. E. and Arakawa, Y., "Optimization of current Distribution in an Applied-Field MPD Thruster," Proceedings of 20th International Electric Propulsion Conference, 1988, pp. 323-332.
6. Bishaev, A. M. and Kim, V., "Local plasma properties in a Hall-current accelerator with an extended acceleration zone," Soviet Physics-Technical Physics, Vol. 23, 1978, pp. 1055-1057.
7. Kaufman, H. R., "Theory of Ion Acceleration with Closed Electron Drift," Journal of Spacecraft and Rockets, Vol. 21, No. 6, 1984, pp. 558-562.
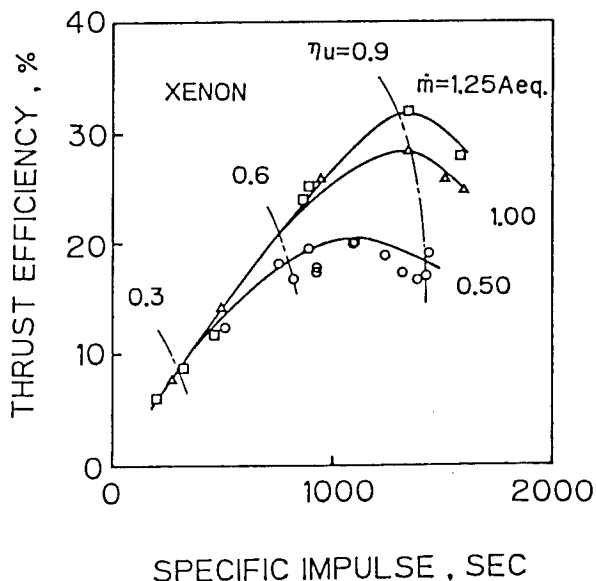
Fig. 7 Thruster performance obtained by Thruster II when xenon is used as the propellant
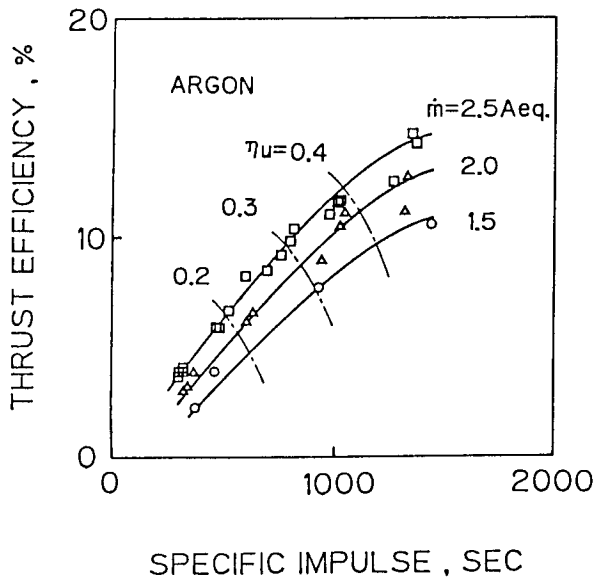

Fig. 8 Thruster performance obtained by Thruster II when argon is used as the propellant